Electronic Supplementary Material (ESI) for ChemComm.

Supporting Information

H-Bonding and Charging Mediated Aggregation and Emission for Fluorescence Turn-on Detection of Hydrazine Hydrate

Deyan Zhou,[†] Yangyang Wang,[†,‡] Jiong Jia,[†] Wenzhu Yu,[†] Baofeng Qu,[†] Xia Li,[†] Xuan Sun[†]*

[†]*Key Laboratory for Colloid & Interface Chemistry, Shandong University, Education Ministry, Jinan, 250100, P. R. China*

[‡]*State Key Lab of Crystal Materials, Shandong University, Jinan, 250100, P. R. China*

E-mail: sunxuan@sdu.edu.cn

Content

1. Experimental section: Synthesis and characterization

1.1 Instruments and measurements

^{1}H NMR spectra was recorded on a Bruker DPX 300 spectrometer (300 MHz) using TMS as an internal reference. ^{13}C NMR spectra was obtained on a Bruker AVANCE 400 spectrometer (100 MHz). Matrix-assisted laser desorption/ionization time-of-flight (MALDI-TOF) mass spectra was captured on a Bruker BIFLEXIII ultrahigh-resolution. Absorption spectra were obtained on a Hitachi U-4100 spectrophotometer. Fluorescence lifetimes were measured on an FLS920 (Edinburgh) fluorometer by time correlated single photon counting (TSPC). The absolute fluorescent quantum yields were determined with integrating spheres on FLS920. FT-IR measurements were recorded for KBr pellets with a resolution of 2 cm^{-1} using a VER-TEX-70 (Bruker) spectrometer. Transmission electron microscopy (TEM) images were recorded on a JEOL-100CX II electron microscope operating at 100 kV. For TEM, a drop of sample solution was cast onto a copper grid prayed with carbon. The powder X-ray diffraction (XRD) patterns were recorded using a Rigaku D/Max 2200-PC diffractometer with Cu-Ka radiation (λ = 0.15418 nm) and a graphite monochromator at ambient temperature. Confocal fluorescent microscopy (CFM) images were conducted on FV 500 (OLYMPUS) microscopy excited with 400 nm.

CV measurements were performed in a one-compartment cell containing a solution of **1** (2 mM) in dry DMSO in the presence of tetra-n-butylammonium hexafluorophosphate (0.1 M) using a Model CH1760D potentiostat–galvanostat under computer control. The working electrode was Pt wire with a diameter of 1 mm, and the counter electrode was glassy carbon electrode. An $Ag/AgNO_3$ ($0.01M/CH_3CN$) electrode directly immersed in the solution served as the reference electrode. Tests were carried out at a scan rate of 10 mV s^{-1} at room temperature under nitrogen.

Electron Paramagnetic Resonance (EPR) Spectroscopy were obtained from State Key Laboratory of Structural Chemistry, Fujian Institute of Research on the Structure of Matter. EPR spectra were conducted on a Bruker E-500 spectrometer, at the X-band, microwave frequency 9.8 GHz; microwave power 1.5 db; and modulation amplitude

0.5 Gauss (G) at 298 K. The microwave frequency was measured with a built-in digital counter. Modulation amplitude and microwave power were optimized for high signal-to-noise ratio and narrow peaks.

1.2 Computational Details: Quantum-chemical calculations were performed on **1** using Gaussian 09. The geometry of **1** was optimized using Becke's three-parameter and Lee-Yang-Parr hybrid functional (B3LYP) and a 6-31g (d) basis set. Following this, Time-dependent density functional theory (TD-DFT) calculations were carried out on the optimized molecular structure in order to determine the photoexcitation mechanism of **1**.

1.3 Synthetic procedure

1.3.1 Synthesis of compound AB-NDI 1.

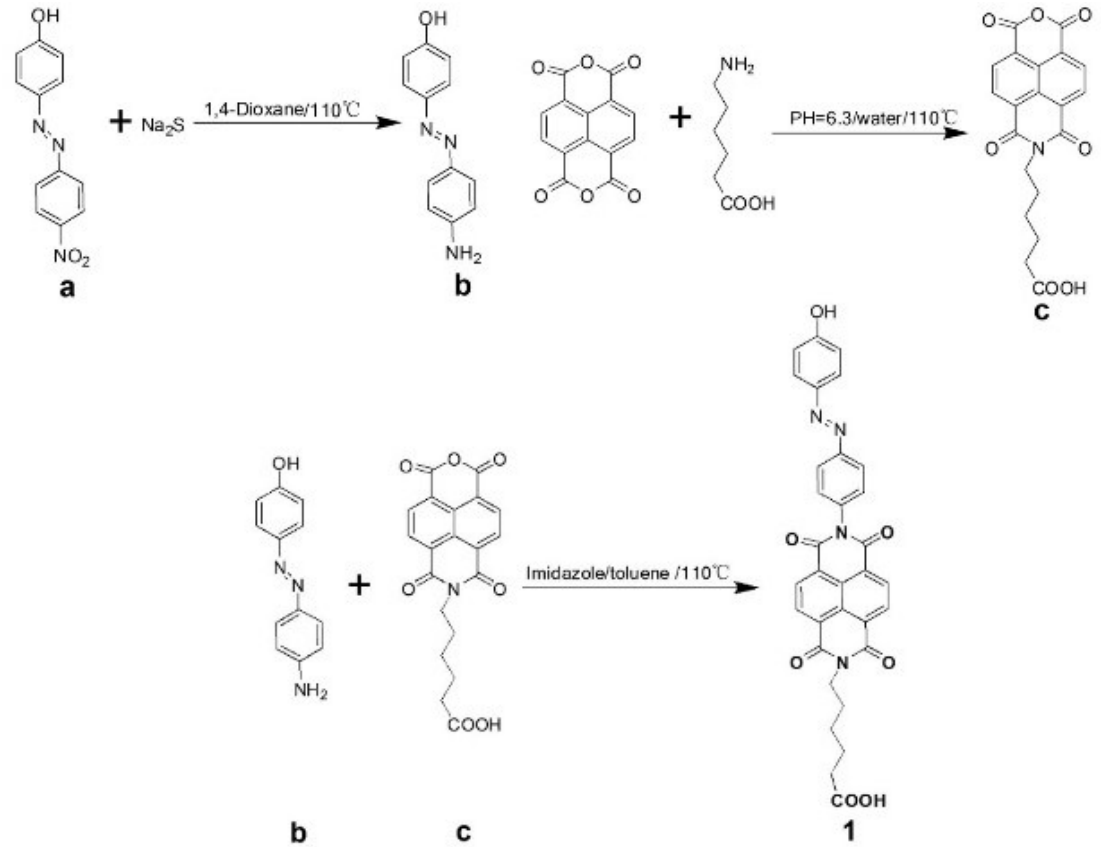

Scheme S1. Synthesis of AB-NDI **1**

4-((4-nitrophenyl)diazenyl)phenol (a)[1-2]

4-Nitroaniline (4 g, 0.029 mol) was added to the hydrochloric acid aqueous solution

(10%, 66 ml) and was stirred until dissolved. Sodium nitrite (2.58 g, 0.037 mol) was dissolved in 55 mL water and was added dropwise to the above solution within 1 h, then stirred for another 30 minutes, keeping the temperature under 2ºC. Phenol (3.48 g, 0.037 mol) and sodium hydroxide (1.48 g, 0.037 mol) were dissolved in water (40 ml), and the mixture was added dropwise to the above diazonium salt solution within 1 h, keeping the temperature under 2ºC. The reaction was completed after stirring for another 3 h under 2ºC. After stewing at room temperature for 24 h, an orange product was precipitated and collected by filtration. The product was pure enough without further purification with yield of almost 100% (7g). ^{1}H NMR (300 MHz, DMSO-d6, ppm): δ 6.97-7.00 (d, *J* = 8.7 Hz, 2H, benzene), 7.88-7.91 (d, *J* = 9.0 Hz, 2H, benzene), 7.99-8.02 (d, *J* = 8.7 Hz, 2H, benzene), 8.39-8.42 (d, *J* = 9.0 Hz, 2H, benzene), 10.61 (s, 1H, -OH), MS *m/z*: Observed 242.0545 M^-, M^-_{calcd} = 242.06

4-((4-aminophenyl)diazenyl)phenol (b)[2]

a (0.729g, 0.003 mol), Na_2S (1.5g, 0.0192 mol) were dissolved in mixed solvent of 90 mL dioxane and 9 mL water, then stirred and reacted at temperature of 90ºC for four hours. After 100 mL saturated solution of sodium bicarbonate was added, the mixture was extracted with CH_2Cl_2 (3 × 100 mL). The organic layers were combined and collected, dried over $MgSO_4$, and evaporated in vacuum to afford orange solid. The crude product was purified by chromatography, eluting with solvent (EtOAc/PE, 1:2 v/v). Orange solid was collected (0.55g, 86% yield). ^{1}H NMR (300 MHz, DMSO-d6, ppm): δ 5.90 (s, 2H, $-NH_2$), 6.63-6.66 (d, *J* = 8.7 Hz, 2H, benzene), 6.85-6.88 (d, *J* = 9.0 Hz, 2H, benzene), 7.56-7.59 (d, *J* = 8.7 Hz, 2H, benzene), 7.62-7.65 (d, *J* = 8.7 Hz, 2H, benzene), 9.95 (s, 1H, -OH), MS *m/z*: Observed 214.1016 $[M+H]^+$, $[M+H]^+_{calcd}$ = 214.09

6-(1,3,6,8-tetraoxo-1H-isochromeno[6,5,4-def]isoquinolin-7(3H,6H,8H)-yl)hexanoic acid (c)[3,4]

1,4,5,8-naphthalene-tetracarboxylic dianhydride (NTCDA, 0.4g, 1.49 mmol) was dispersed into 65 mL water. After 7 mL 1mol/L KOH aqueous solution was added, the solution became transparent with yellow color. The pH was adjusted to 6.3 using

1mol/L H_3PO_4 aqueous solution, then 6-aminocaproic acid aqueous solution (0.1954g/5mL water) was added. After the solution was refluxed at 110ºC for 12h, the PH was adjusted to 1~2 using 2M HCl aqueous solution with white solids appeared. The solids were collected by filtration and washed with water. The white solid was dispersed into 100 mL acetic anhydride, then refluxed at 110ºC under the protection of N_2 until all solids are dissolved. After removing acetic anhydride in vacuum, the solid was dispersed into 100mL water under ultrasonic wave and collected by filtration to get the brown solids (0.3527g, 62.1% yield). ^{1}H NMR (300 MHz, DMSO-d6, ppm): δ 1.37-1.45 (m, 2H, -CH_2), 1.53-1.73 (m, 4H, -CH_2), 2.50-2.56 (t, *J* = 7.2 Hz, 2H, -CH_2), 4.04-4.08 (t, *J* = 7.2 Hz, 2H, -CH_2), 8.70 (s, 4H, naphthalene), 11.99 (s, 1H, -COOH), MS *m/z*: Observed 380.0743 M^-, M^-_{calcd} = 380.08

6-(7-(4-((4-hydroxyphenyl)diazenyl)phenyl)-1,3,6,8-tetraoxo-7,8-dihydrobenzo[lmn][3,8]phenanthrolin-2(1H,3H,6H)-yl)hexanoic acid (1)[3,5].

B (0.256g, 1.2 mmol), **C** (0.381g, 1 mmol), and imidazole (3g) were dissolved in 120 mL distilled toluene, then refluxed at 110ºC the protection of N_2 for two days. Then solvent was evaporated in vacuum to afford orange solid. The solid was dissolved with CH_2Cl_2, then washed with water for three times to remove imidazole. The organic layer was evaporated in vacuum to afford a yellow solid. The crude product was purified by chromatography, eluting with solvent (CH_2Cl_2/CH_3OH, 100:8 v/v). Yellow solids (95 mg, 16.5% yield). ^{1}H NMR (300 MHz, DMSO-d6, ppm): δ 1.39-1.41 (m, 2H, -CH_2), 1.55-1.59 (m, 2H, -CH_2), 1.67-1.69 (m, 2H, -CH_2), 2.16-2.21 (t, *J* = 6.9 Hz, 2H, -CH_2), 4.04-4.08 (t, *J* = 7.2 Hz, 2H, -CH_2), 6.94-6.97 (d, *J* = 8.7 Hz, 2H, benzene), 7.60-7.63 (d, *J* = 8.4 Hz, 2H, benzene), 7.82-7.85 (d, *J* = 8.7 Hz, 2H, benzene), 7.94-7.97 (d, *J* = 8.4 Hz, 2H, benzene), 8.69 (s, 4H, naphthalene), 10.40 (s, 1H, -OH), 12.02 (s, 1H, -COOH). ^{13}C NMR (100 MHz, DMSO-d6, ppm): δ 24.74, 26.53, 27.63, 34.10, 116.49, 122.95, 125.49, 126.69, 126.86, 127.04, 127.29, 130.61, 130.92, 137.63, 145.74, 152.39, 161.79, 163.05, 163.30, 174.97. MS *m/z*: Observed 577.1622 $[M+H]^+$, $[M+H]^+_{calcd}$ = 577.16

1.3.2 Synthesis of control compound COOH-NDI 2.

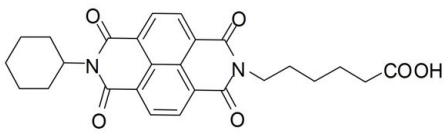

2

Scheme S2. Molecular structure of compound **2**

6-(7-cyclohexyl-1,3,6,8-tetraoxo-7,8-dihydrobenzo[lmn][3,8]phenanthrolin-2(1H,3H,6H)-yl)hexanoic acid (2)

Compound **2** was synthesized according to the synthetic procedure of **1**. ^{1}H NMR (300 MHz, DMSO-d6, ppm): δ 0.85-1.87(m, 16H, -CH_2), 2.20-2.25 (t, J = 7.2 Hz, 2H, -CH_2), 4.02-4.07 (t, J = 7.2 Hz, 2H, -CH_2), 4.84-4.92 (t, J = 12.0 Hz, H, -CH), 8.66 (s, 4H, naphthalene), 11.99 (s, 1H, -COOH). MS *m/z*: Observed 463.1756 $[M+H]^+$, $[M+H]^+_{calcd}$ = 463.18

1.3.3 Synthesis of compound OH-AB 3.

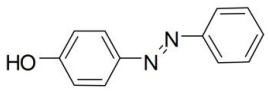

3

Scheme S3. Molecular structure of compound **3**

4-(phenyldiazenyl)phenol (3)

Compound **3** was synthesized according to the synthetic procedure of **a**.

^{1}H NMR (300 MHz, DMSO-d6, ppm): δ 6.92-6.96 (d, J = 8.7 Hz, 2H, benzene)，7.47-7.59 (m, 3H, benzene), 7.79-7.83 (d, J = 9.0 Hz, 4H, benzene), 10.31 (s, 1H, -OH). MS *m/z*: Observed 197.0876 M^-, M^-_{calcd} = 197.08

References

S1. F. Hamon, F. Djedaini-Pilard, F. Barbot and C. Len, *Tetrahedron*, 2009, **65**, 10105.

S2. I. Cârlescu, A. M. Scutaru, D. Apreutesei, V. Alupei and D. Scutaru, Liquid Crystals, 2007, **34**, 775.

S3. S. V. Bhosale, C. H. Jani and S. J. Langford, *Chem. Soc. Rev.*, 2008, **37**, 331.

S4. T. Helmat, *Dye and Pignients*, 1983, **4**, 171-174.

S5. F. W. Harris, S. H. Lin, F. Li, *Polymer*, 1996, **37**, 5049-5057.

2. UV-vis spectra and Fluorescence spectra of 1, 2 and 3 in DMSO

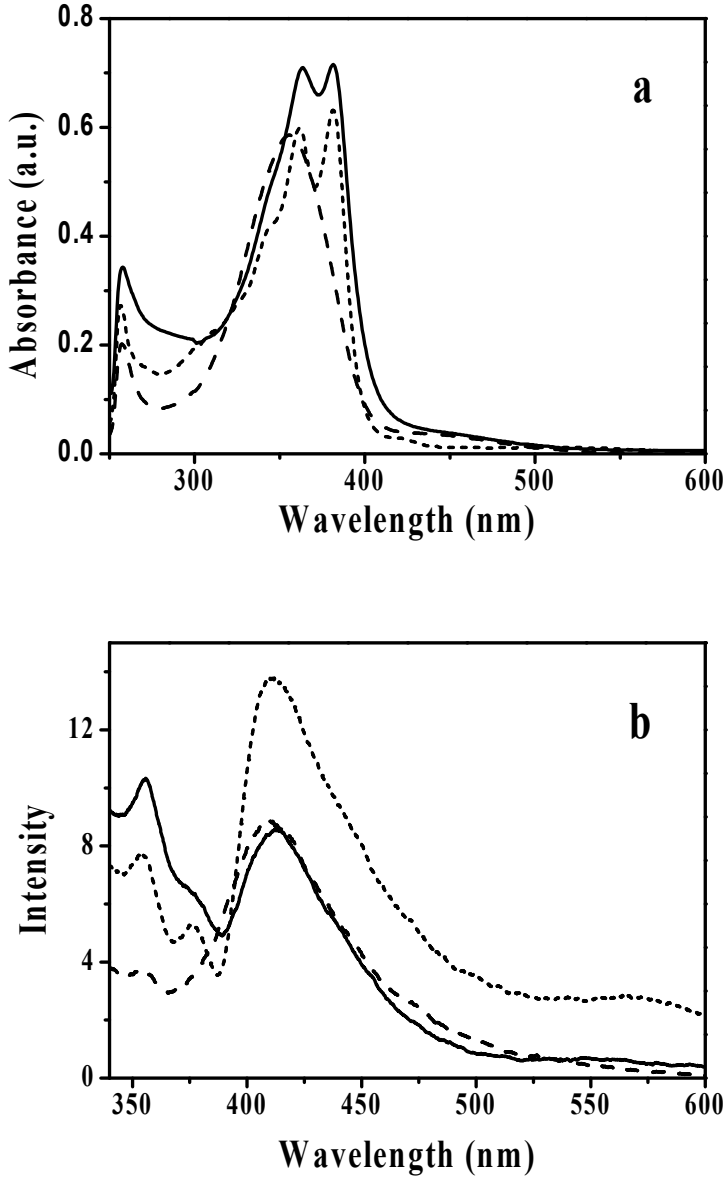

Fig. S1. (a) UV-vis spectra and (b) fluorescence spectra of compound **1** (solid line), the control compounds COOH-NDI **2** (short-dashed line) and OH-AB **3** (dashed line) in DMSO, excited by 320 nm, with concentration of 25μM.

3. Cyclic voltammetry (CV) of 1 in DMSO

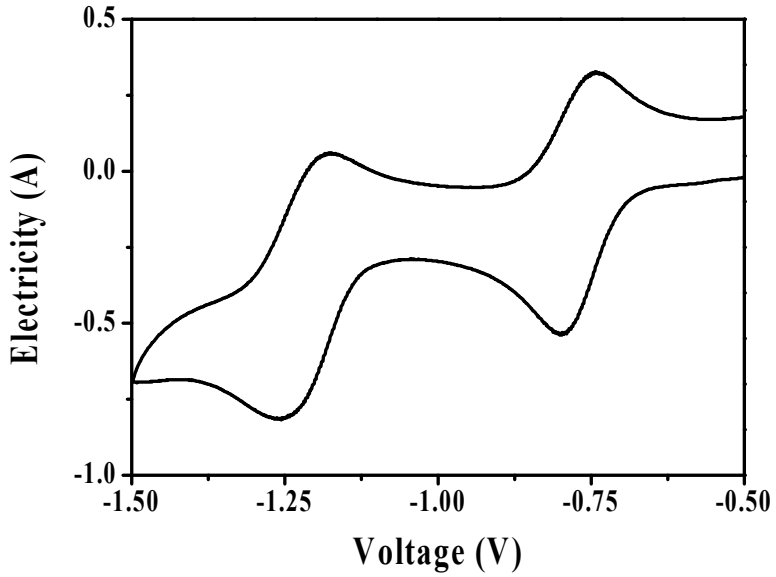

Fig. S2. Cyclic voltammetry (CV) of compound **1** in DMSO (2 mM) with 0.1 M TBAP supporting electrolyte.

4. TEM of aggregates of 1

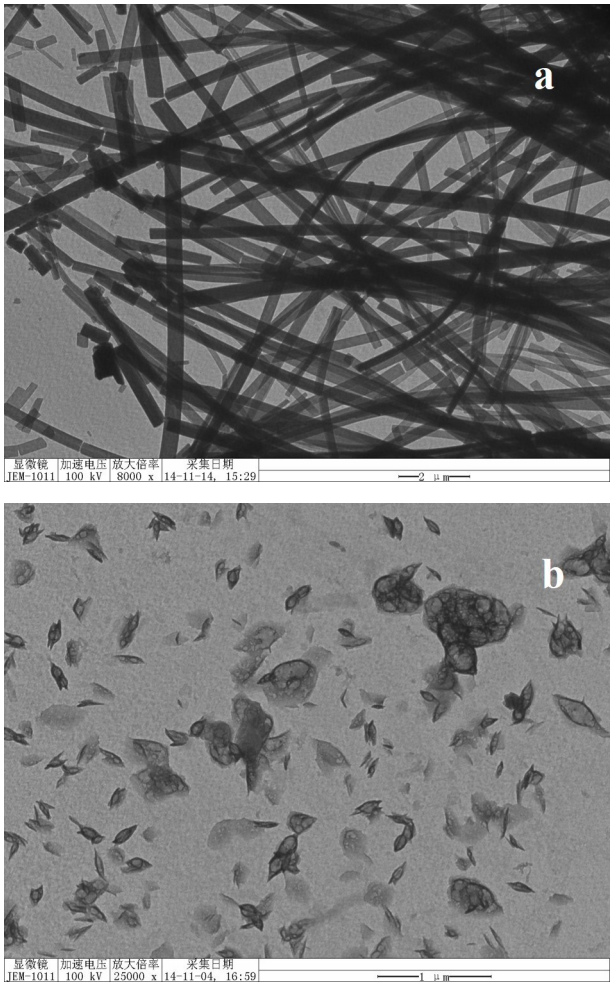

Fig. S3. TEM observation of the aggregates of **1** (a) before and (b) after adding hydrazine hydrate.

5. FT-IR characterization of the intermolecular hydrogen-bonding

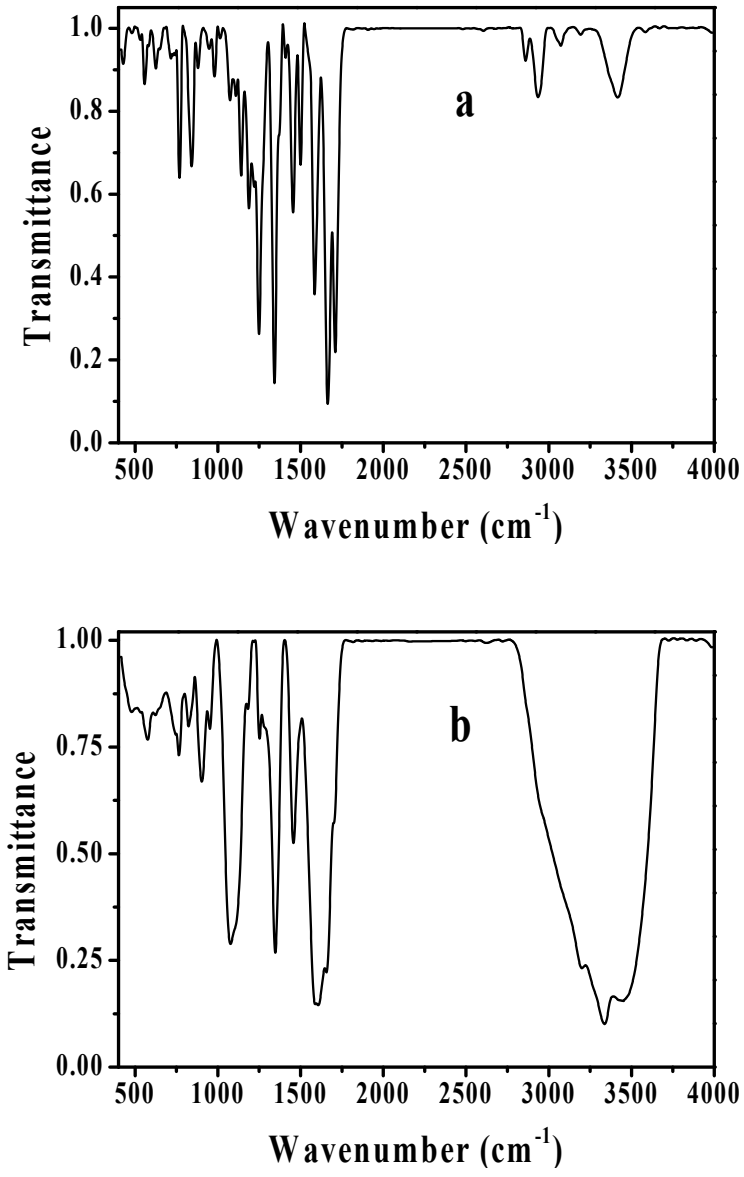

Fig. S4. FT-IR spectra of the aggregates before (a) and after (b) NH_2-NH_2 was added.

6. The XRD pattern of the aggregates of 1

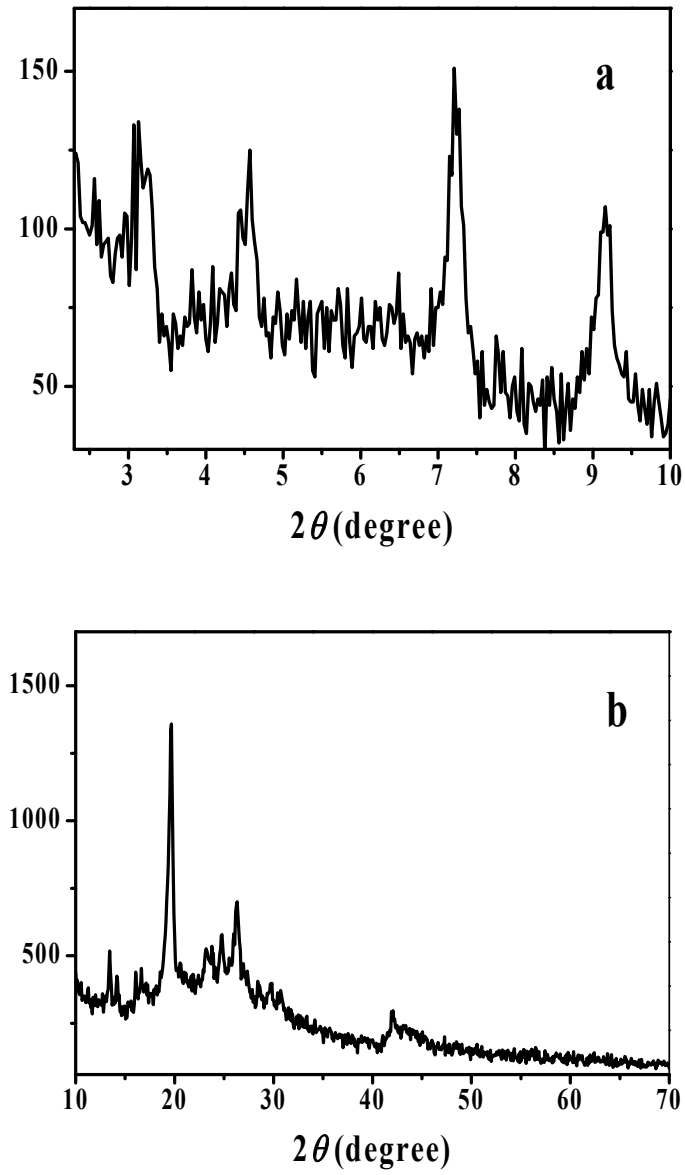

Fig. S5. (a) Small (SAXRD) and (b) wide angle XRD (WAXRD) pattern of the nanoribbons of **1**

7. UV-vis absorption of 2 and 3 with different amounts of hydrazine hydrate

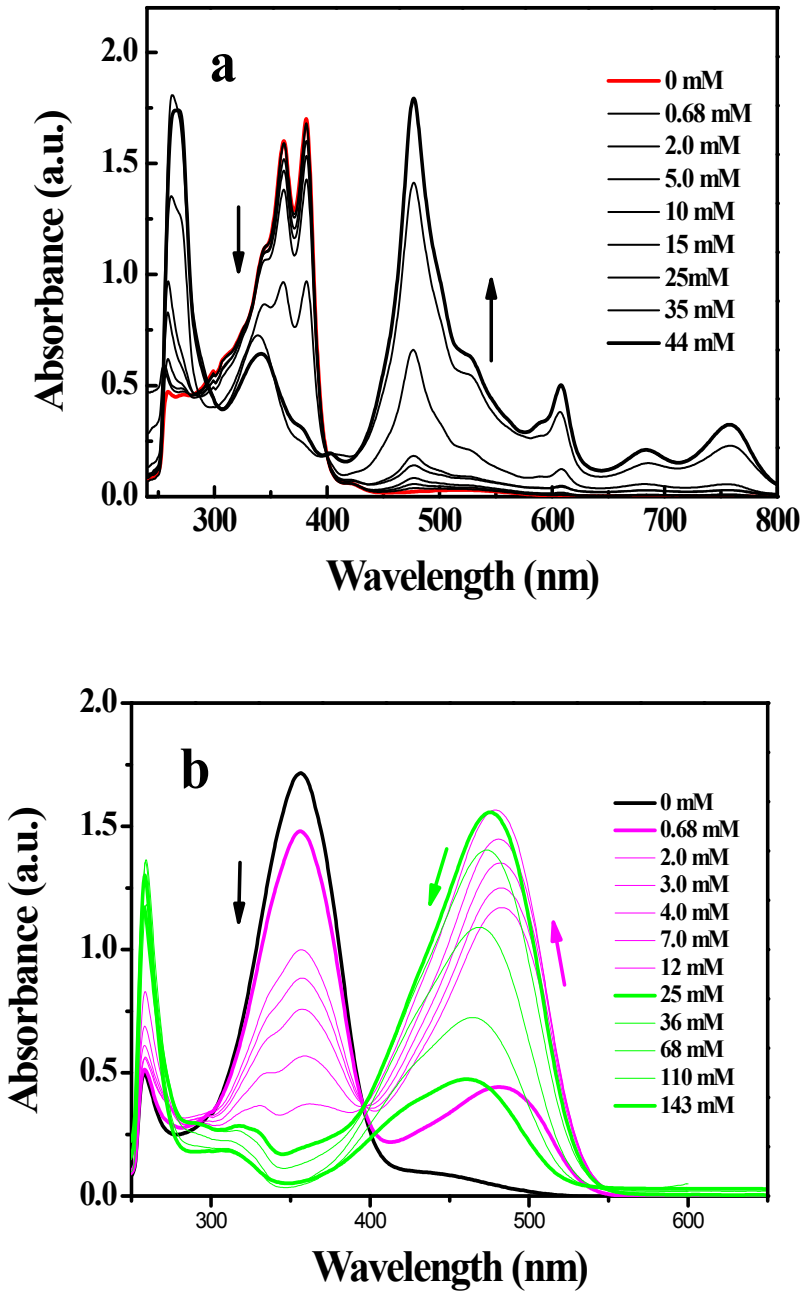

Fig. S6. UV-vis absorption spectra of (a) compound **2** and (b) **3** in DMSO (25μM) with addition of hydrazine hydrate.

8. [1]H-NMR spectrum of the hydrazine hydrate addition products

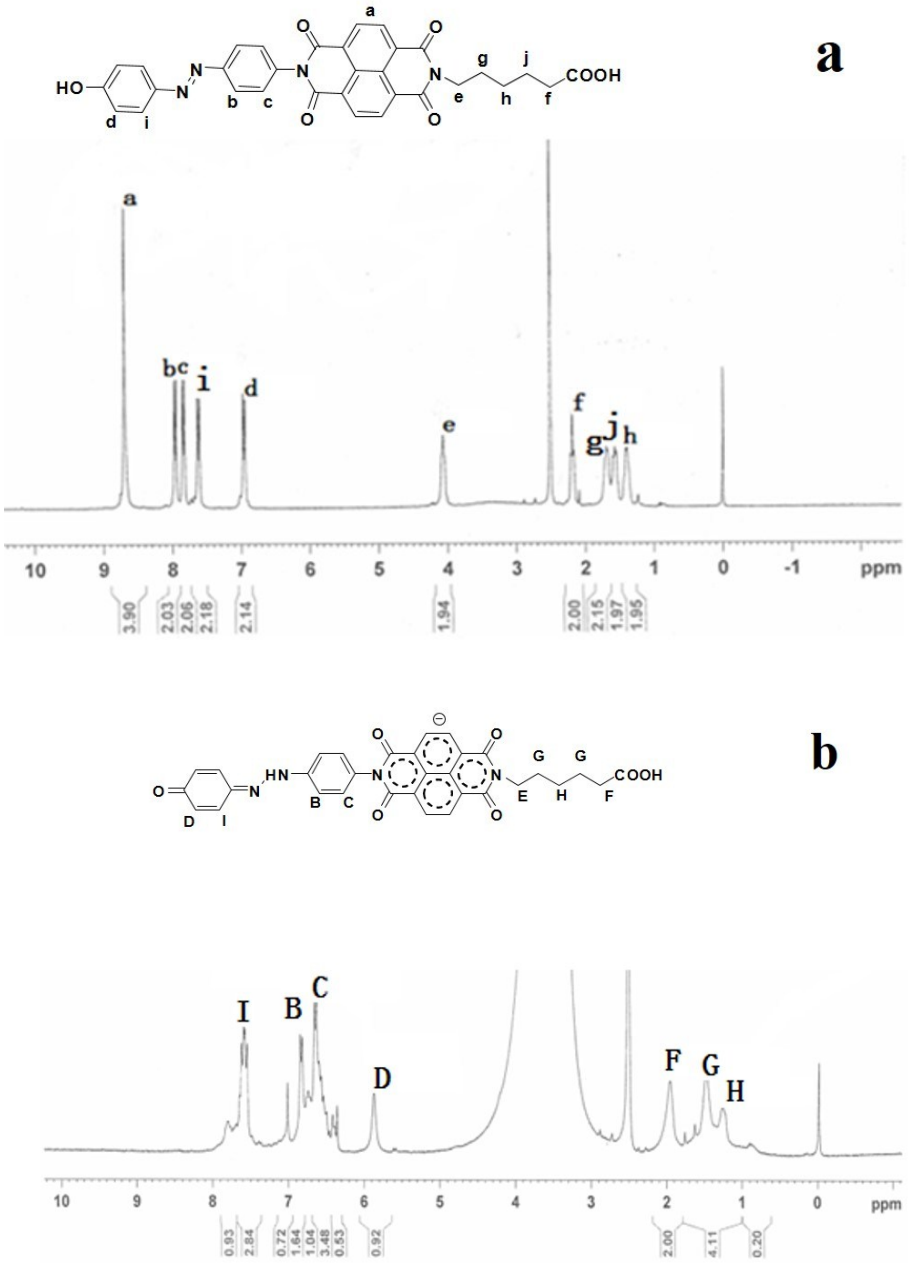

Fig. S7. [1]H-NMR spectrum of the (a) compound **1** and (b) hydrazine hydrate addition product

9. Electron paramagnetic resonance (EPR) of 1 before and after adding hydrazine hydrate

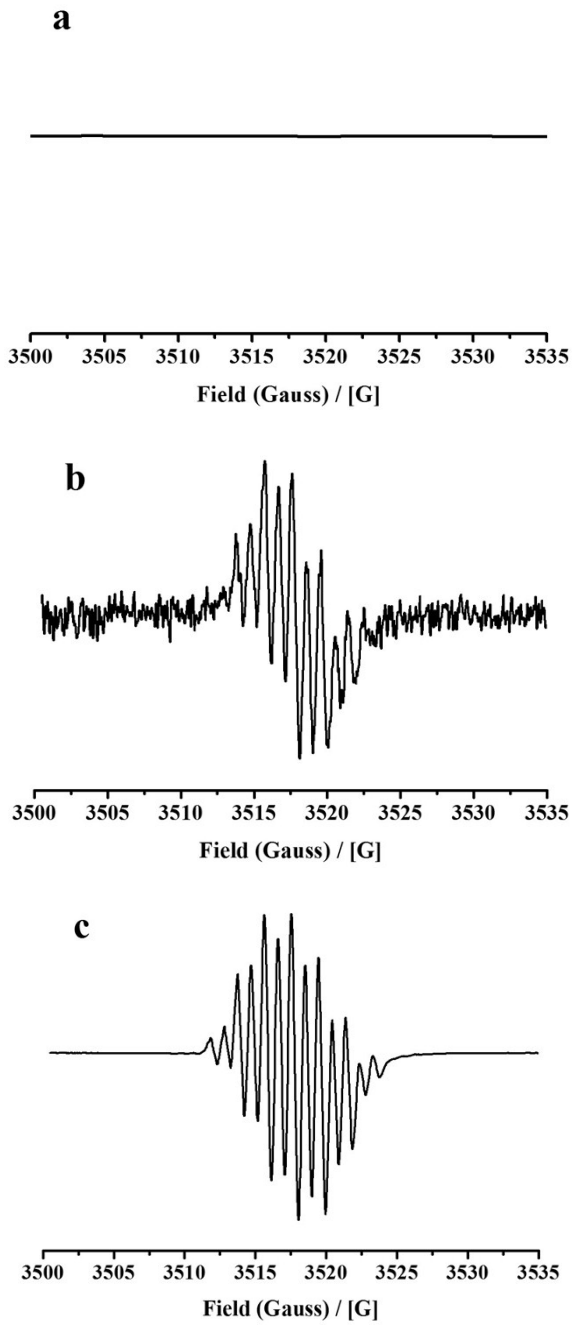

Fig. S8. The EPR spectrum of **1** (1 mM / DMSO) in the absence of hydrazine (a), in presence of 1 equiv of hydrazine (b), and in presence of 30 equiv of hydrazine (c) at room temperature. Both (b) and (c) spectra show hyperfine splitting pattern indicating the formation of delocalized $NDI^{\bullet-}$ radical anion (g = 2.0038).

10. Excition spectra of 1 in DMSO and the aggregates at the presence of hydrazine hydrate

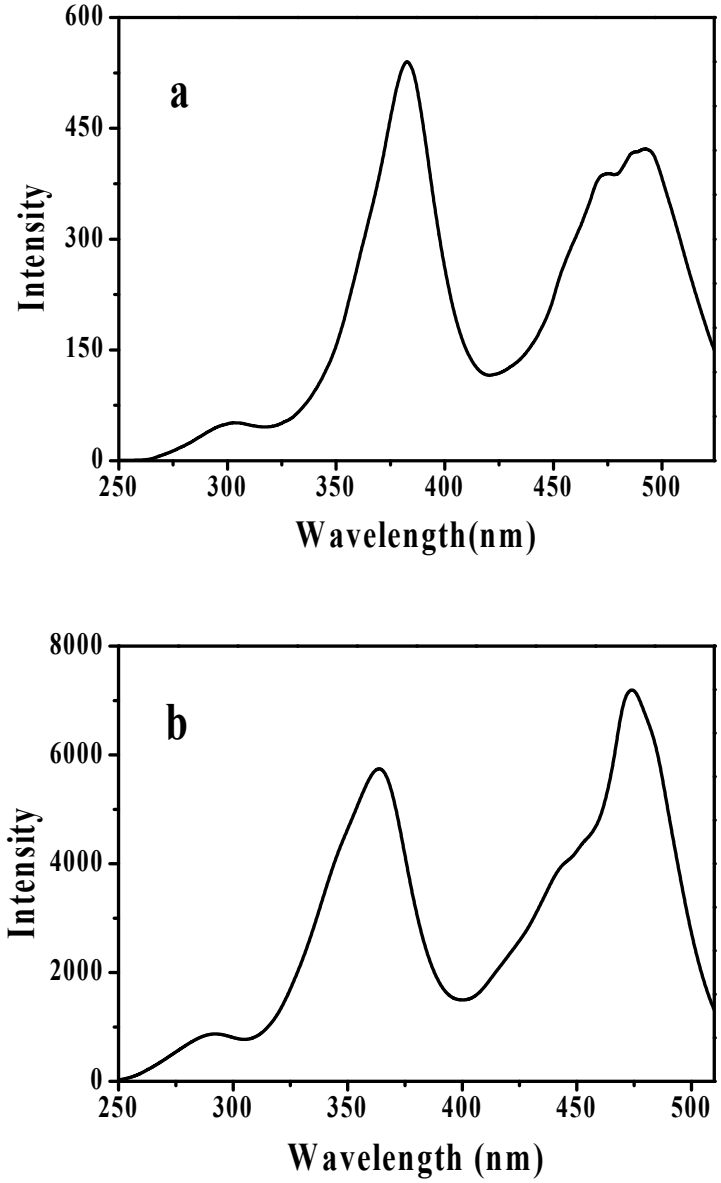

Fig. S9. The excition spectra of (a) **1** (25 μM / DMSO) in presence of 20 equiv of hydrazine hydrate, and (b) the aggregates with 20 equiv of hydrazine hydrate

11. TDDFT calculation results of 1 and the hydrazine hydrate addition product

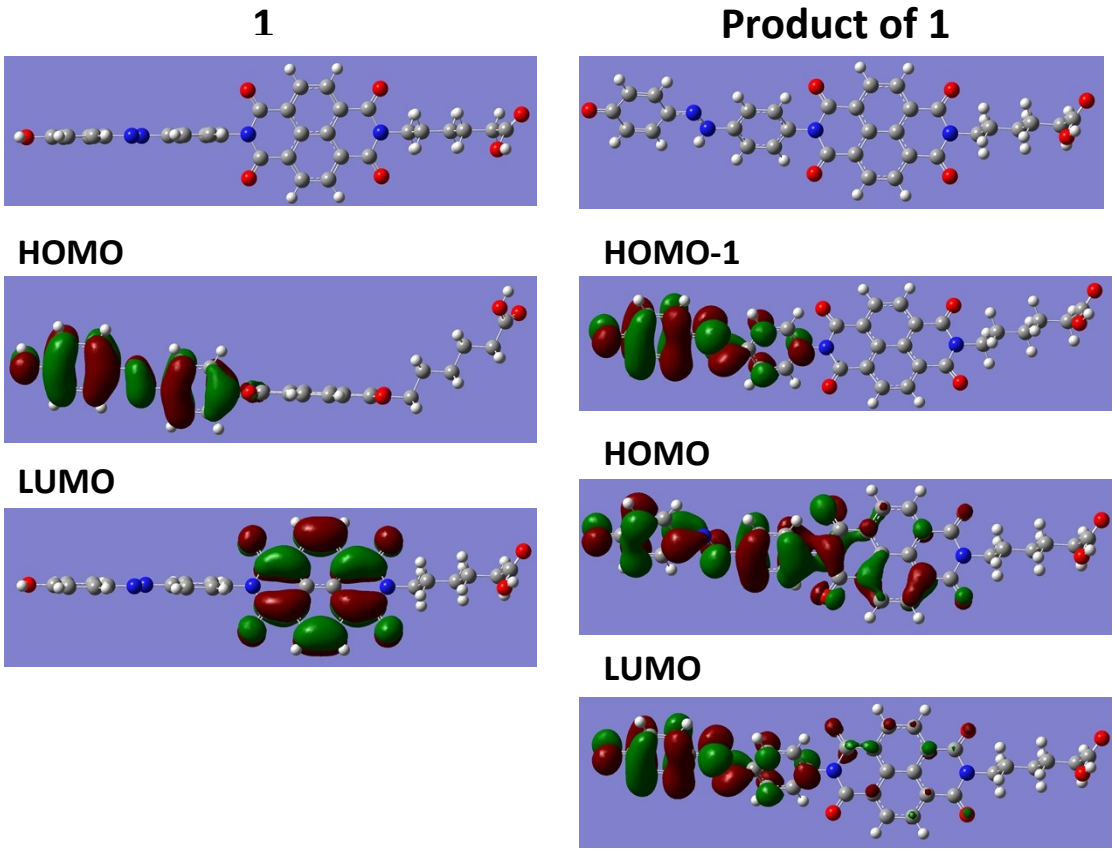

Fig. S10. Frontier molecular orbitals of **1** and the hydrazine hydrate addition product.

12. UV-vis absorption and fluorescence spectra of 1 with a variety of other related test species

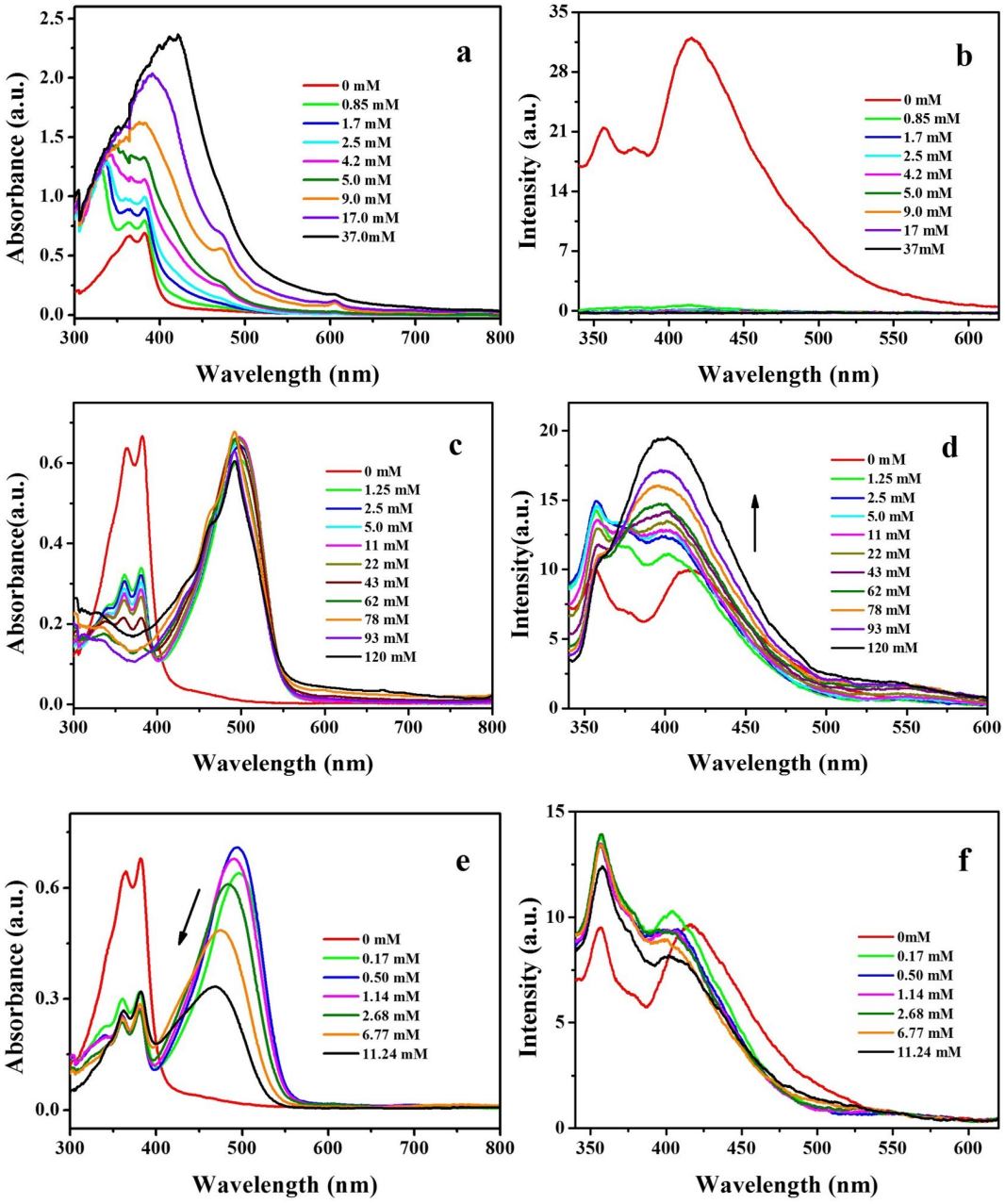

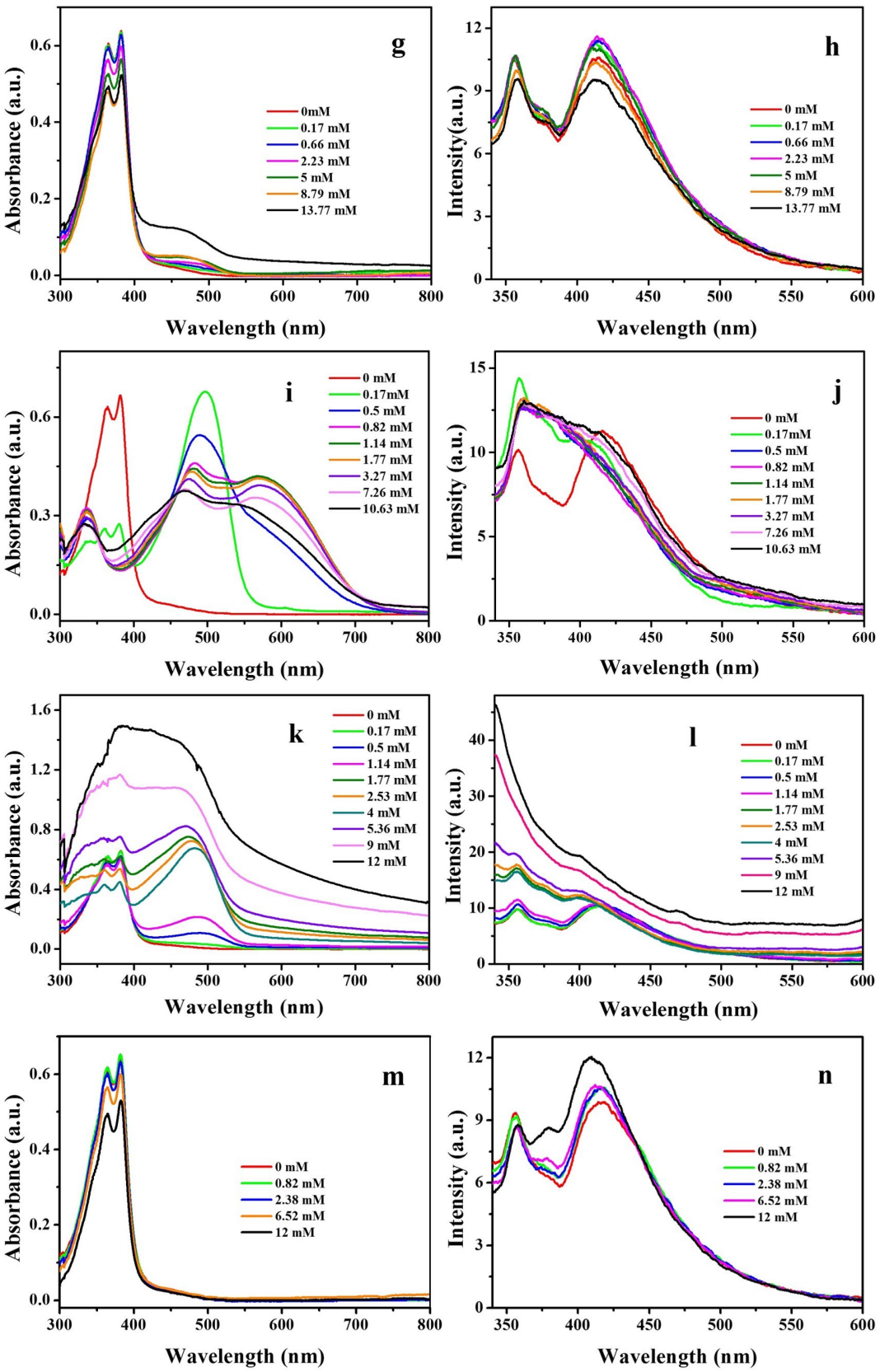
g
Absorbance (a.u.)
Wavelength (nm)
0mM
0.17 mM
0.66 mM
2.23 mM
5 mM
8.79 mM
13.77 mM
h
Intensity(a.u.)
Wavelength (nm)
0 mM
0.17 mM
0.66 mM
2.23 mM
5 mM
8.79 mM
13.77 mM
i
Absorbance (a.u.)
Wavelength (nm)
0 mM
0.17mM
0.5 mM
0.82 mM
1.14 mM
1.77 mM
3.27 mM
7.26 mM
10.63 mM
j
Intensity (a.u.)
Wavelength (nm)
0 mM
0.17mM
0.5 mM
0.82 mM
1.14 mM
1.77 mM
3.27 mM
7.26 mM
10.63 mM
k
Absorbance (a.u.)
Wavelength (nm)
0 mM
0.17 mM
0.5 mM
1.14 mM
1.77 mM
2.53 mM
4 mM
5.36 mM
9 mM
12 mM
l
Intensity (a.u.)
Wavelength (nm)
0 mM
0.17 mM
0.5 mM
1.14 mM
1.77 mM
2.53 mM
4 mM
5.36 mM
9 mM
12 mM
m
Absorbance (a.u.)
Wavelength (nm)
0 mM
0.82 mM
2.38 mM
6.52 mM
12 mM
n
Intensity (a.u.)
Wavelength (nm)
0 mM
0.82 mM
2.38 mM
6.52 mM
12 mM

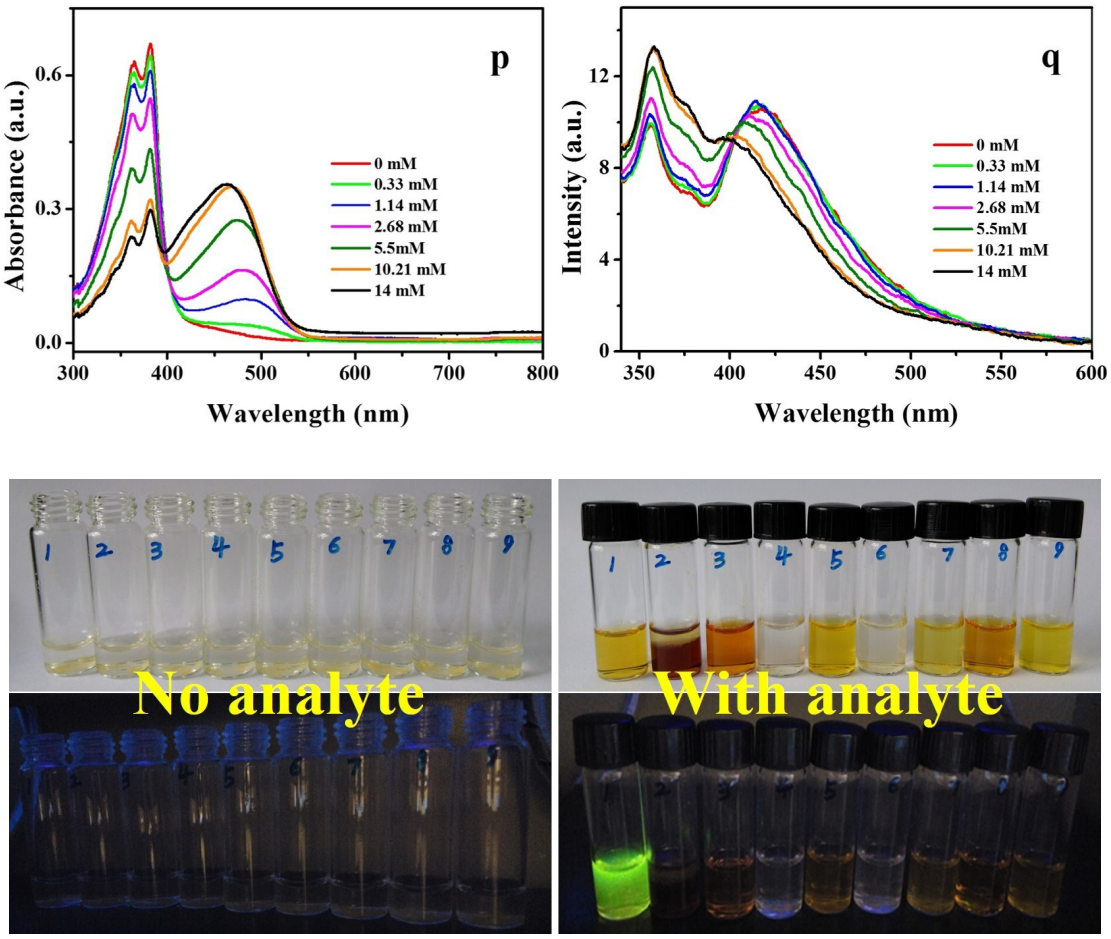

Fig. S11. Absorption and fluorescence spectra with addition of phenyl hydrazine (a) and (b); ethylenediamine (c) and (d); F^- (e) and (f); I^- (g) and (h); S^{2-} (i) and (j); SO_3^{2-} (k) and (l); hydroxylamine hydrochloride (m) and (n); ammonium hydroxide (p) and (q). The photographs demonstrate the changes of the aggregates before and after adding 1. hydrazine, 2. phenyl hydrazine 3. ethylenediamine, 4. Hydroxylamine hydrochloride 5. $NH_3 \bullet H_2O$, 6. F^-, 7. I^-, 8. S^{2-}, and 9. SO_3^{2-}, respectively, indicating the selectivity toward hydrazine.

13. UV-vis absorption and fluorescence spectra of aggregates with hydrazine hydrate

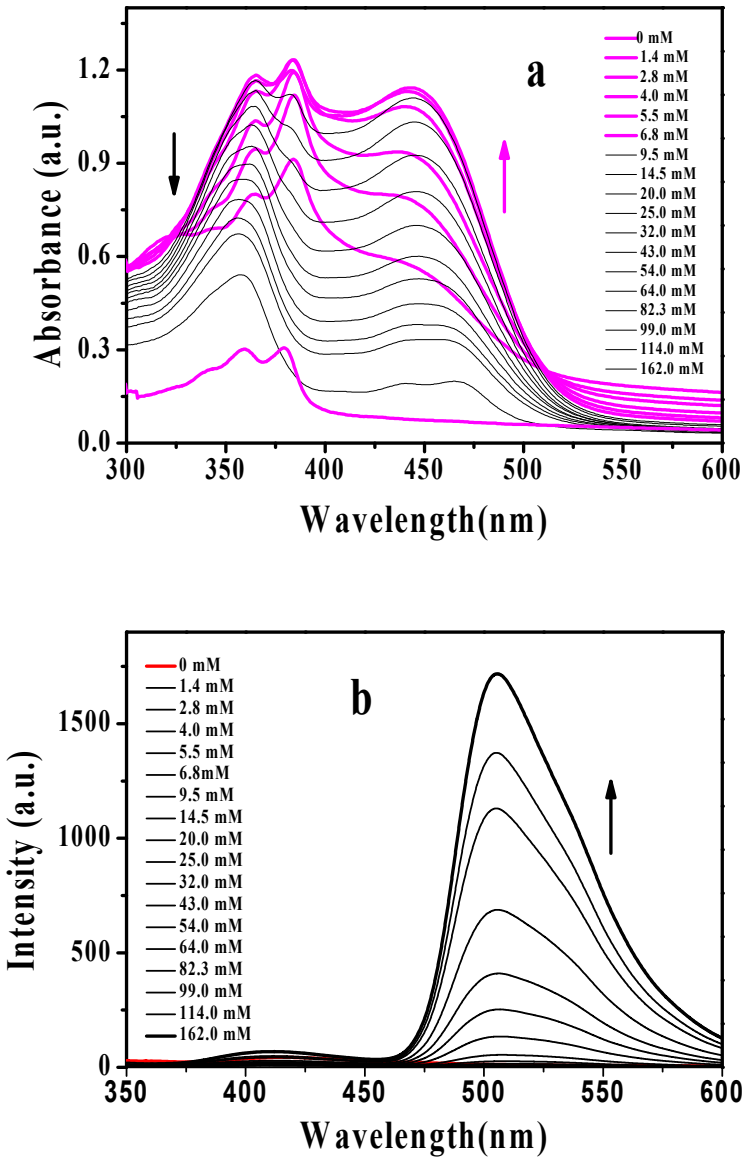

Fig. S12. (a) UV-vis absorption spectra and (b) fluorescence spectra of aggregates with addition of hydrazine hydrate.

14. TEM and the fluorescence spectra of the nanoribbons after F^- was added

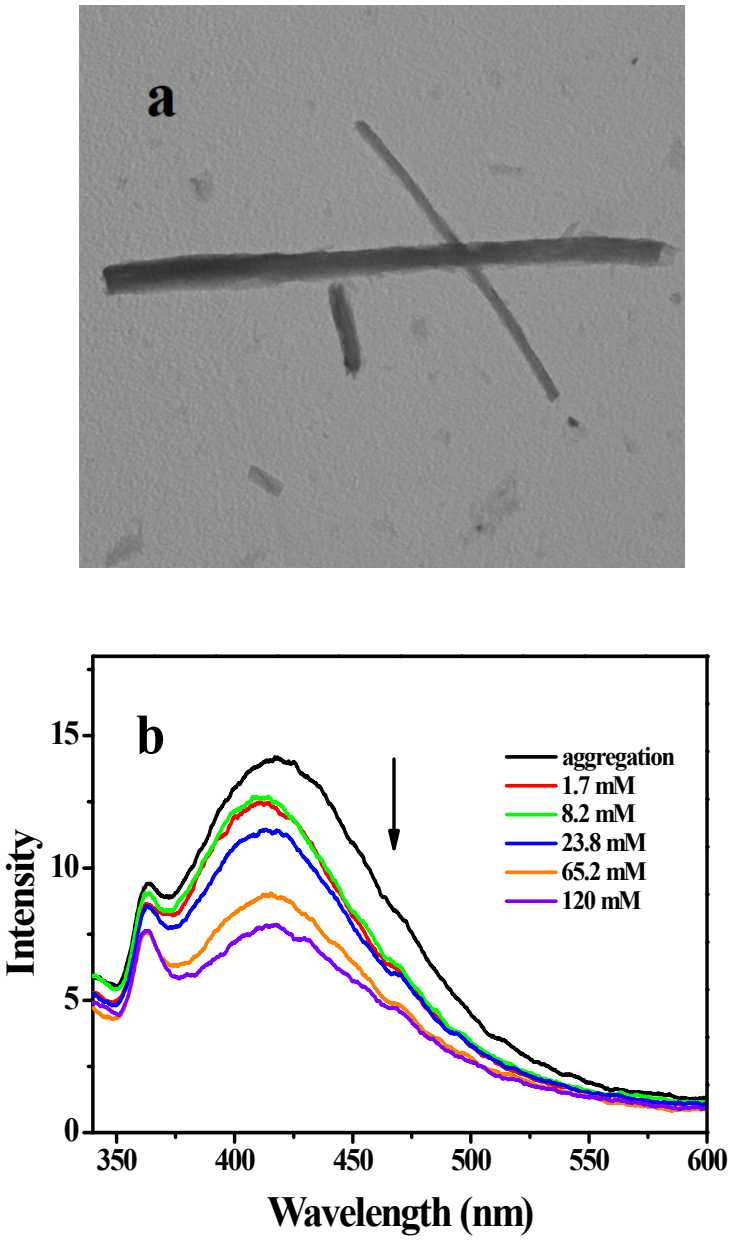

Fig. S13. (a) TEM images and (b) fluorescence spectra of **1** in aggregates after addition of KF.

15. TEM images of aggregates of control compound 2

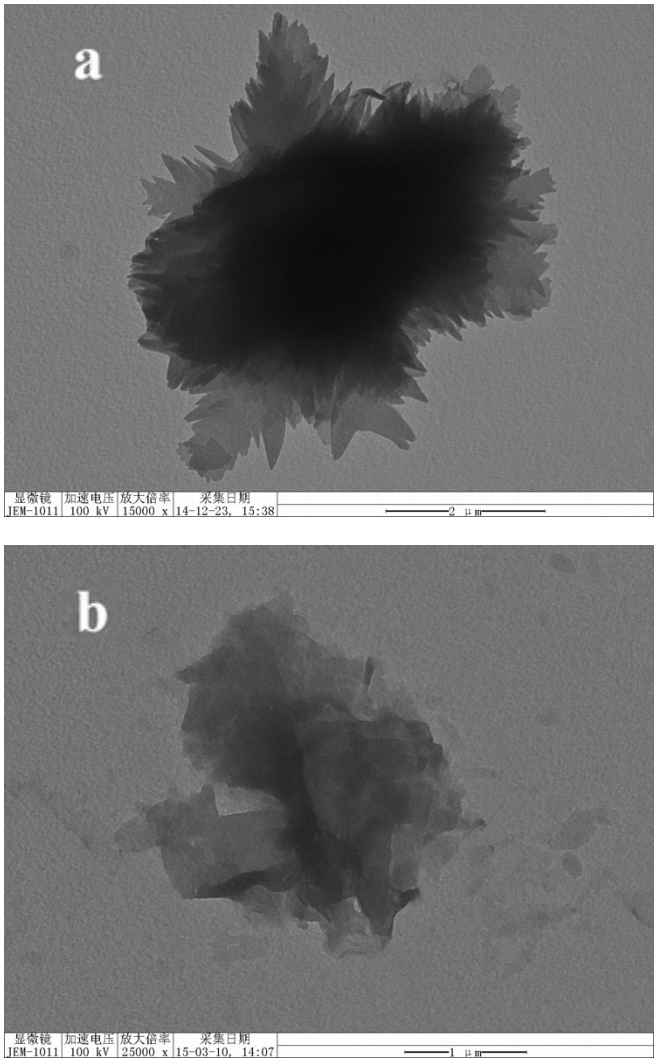

Fig. S14. TEM images of (a) **2** in aggregates and (b) after adding hydrazine hydrate.

.